

# Feasibility Evaluation of the Passive Molten Salt Fast Reactor (PMFR) Concept: A Parametric Sensitivity Analysis of Helical Coil Heat Exchangers and Supercritical Carbon Dioxide Power Conversion Systems

Jihun Im<sup>a</sup>, Jae Hyung Park<sup>a</sup>, Juhyeong Lee<sup>a</sup>, Won Jun Choi<sup>a</sup>, Yun Sik Cho<sup>a</sup>, \*Sung Joong Kim<sup>a, b</sup>.

<sup>a</sup> Department of Nuclear Engineering, Hanyang University, 222 Wangsimni-ro, Seongdong-gu, Seoul 04763, Republic of Korea

<sup>b</sup> Institute of Nano Science and Technology, Hanyang University, 222 Wangsimni-ro, Seongdong-gu, Seoul 04763, Republic of Korea

\* Corresponding author: [sungjkim@hanyang.ac.kr](mailto:sungjkim@hanyang.ac.kr)

## 1. Introduction

The pursuit of reliable and low-carbon energy sources has resulted in a resurgence of interest in alternative energy technologies, including nuclear power. Molten salt reactors (MSRs) have emerged as a promising solution due to their improved efficiency, safety, and high-temperature operation capabilities. However, their commercialization and market demand were impeded by the proliferation risks associated with liquid fuel MSR systems.

To overcome these challenges, the I-SAFE-MSR Research Center in South Korea has developed the Passive Molten Salt Fast Reactor (PMFR) with enhanced safety and versatility features.

The PMFR adopts natural circulation in the reactor loop to eliminate mechanical pumps for hot and radiative fluids [1]. Insoluble fission products are present in MSR's fuel salts because of the fission. These products can cause local heat damage when deposited on structure surfaces. To mitigate this risk, the PMFR are considering using helium bubbling to filter out these elements. The helium injected into the core collects the gaseous precursors and carries the noble metals attached to the interface. This process also potentially enables the natural circulation operation of PMFR. Moreover, the PMFR aims to integrate highly efficient, compact supercritical carbon dioxide (SCO<sub>2</sub>) power conversion systems.

The design of the PMFR's heat exchanger is critical to investigate the feasibility of natural circulation design. The flow rate is directly related to the reactor's power output, and the pressure drop in the heat exchanger significantly hinders the natural circulation flow rate. Additionally, the heat transfer area is a crucial design parameter as excessive heat transfer area can limit the final reactor output, while insufficient heat transfer area can reduce power conversion efficiency.

This study aims to evaluate the feasibility of the PMFR concept by conducting a parametric sensitivity analysis of the heat exchangers and SCO<sub>2</sub> power conversion systems. The analysis involves a performance evaluation of the helical coil heat exchanger, utilizing one-dimensional modeling between the PMFR's natural circulation model and the secondary salt circulation system, with variations in design variables. Subsequently,

the analysis conducts a SCO<sub>2</sub> cycle analysis using the performance evaluation results as input values. Finally, the study compares the electrical output of the PMFR based on the heat exchanger design parameters.

## 2. Modeling of PMFR primary loop

### 2.1 PMFR loop models

The schematic diagram of the PMFR reactor system is illustrated in **Figure 1**. The system comprises a core, a riser, six helical-coil heat exchangers, and a downcomer. Helium is injected into the core from the bottom and travels upwards with the fuel salt, before being separated. As a result, the core and riser experience two-phase flow, while the heat exchangers and downcomers are modeled as single-phase flow. For the separator, a basic cylindrical tank with a metallic mesh screen is assumed.

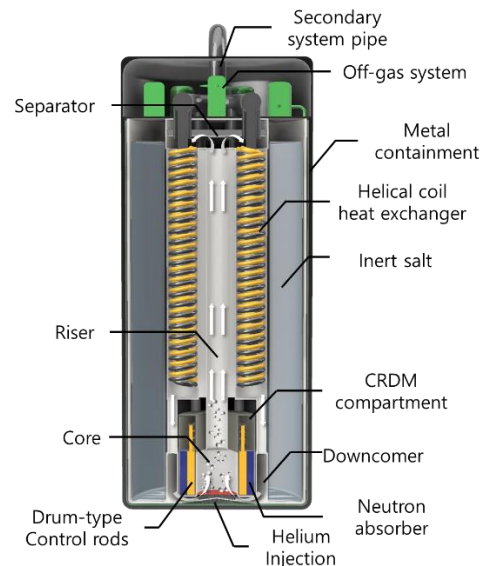


**Figure 1** Schematic diagram of PMFR reactor system

The fuel salt chosen for this study was the UCl<sub>3</sub>-UCl<sub>4</sub>-KCl system, and its thermodynamic properties were obtained from experimental measurements [2–4]. The properties of helium were evaluated using the National Institute of Standards and Technology (NIST) database program. The temperature of helium was assumed to be

the same as the fuel salt, but heat transfer between the two fluids was neglected.

The heat generation of the core was analyzed using a homogeneous cylindrical reactor model, while the decay heat of the fuel was neglected to simplify the analysis.

## 2.2 Hydraulic models for PMFR loop

In this preliminary analysis, the impact of decay heat was disregarded. Consequently, the mass flow rate of the fuel salt was determined based on the energy balance equation.

$$Q = \dot{m} c_p \Delta T \quad (1)$$

The salt circulation cycle in this system can be split into two paths: an upward stream starting from the bottom of the core to the top surface of the separator, and a downward return to the core via the heat exchangers and downcomers. To perform the analysis, each path was nodalized into 100 segments in the z-direction.

Under steady-state conditions, the height level of the salt was fixed. Hence, the velocity of node 1 could be assumed to be zero. Moreover, the pressure at node 1 and 100 in each path was considered identical. This allowed us to derive the pressure balance equations for each path. Here, the index  $i$  denotes the node number and takes a value between 1 and 100.

For upward path,

$$P_n + \sum_i^n (\rho_i g \Delta z) + \sum_i^n P_{loss} = P_i + \left( \frac{1}{2} \rho_i v_i^2 \right)_{t,p} \quad (2)$$

For downward path,

$$P_n + \sum_i^n (\rho_i g \Delta z) = P_i + \left( \frac{1}{2} \rho_i v_i^2 \right) + \sum_i^n P_{loss} \quad (3)$$

Subscripts  $t,p$  means the two-phase flow state.

The core and riser were modeled as the cylindrical pipe, and the two-phase flow friction loss was evaluated by applying Lockhart and Martinelli [5] approach.

$$\Delta P_{t,p} = \Phi^2 \left( f \frac{L}{D} \frac{1}{2} \rho v^2 \right)_{f,superficial} \quad (4)$$

$$\Phi^2 = 1 + \frac{C}{X_{tt}} + \frac{1}{X_{tt}^2} \quad (5)$$

$$X_{tt} = \left( \frac{1-x}{x} \right)^{0.9} \left( \frac{\rho_{He}}{\rho_f} \right)^{0.5} \left( \frac{\mu_f}{\mu_{He}} \right)^{0.1} \quad (6)$$

$X_{tt}$  and  $\Phi$  are Lockhart and Martinelli parameters and the two-phase friction multiplier.

The reduction pressure loss of the flow channel between the core and the riser was evaluated by the following correlation:

$$\Delta P_{reduction} = \left( 1 - \frac{D_{riser}^2}{D_{core}^2} \right) \left( \frac{1}{2} \rho v^2 \right)_{t,p} \quad (7)$$

## 2.3 PMFR heat exchanger models

The PMFR heat exchanger was designated as a helical coil heat exchanger, which is a type of shell-and-tube heat exchanger. Helical coil heat exchangers have been extensively used in compact systems with spatial limitations and have already been integrated into SMRs like SMART and NuScale.

The helical coil heat exchanger consists of a passage for secondary side tubes, a central column that functions as a support for the tube bank, a helical coil tube bank, and a shell that encloses the entire heat exchanger. The arrangement of the tube bank can be either in-lined or staggered.

The PMFR molten salt fuel was designed to flow from top to bottom on the shell side of the mentioned helical coil heat exchanger. This is to reduce the effect of pressure drop in the PMFR loop driven by natural circulation. The secondary side salt was preliminarily designed to flow from the bottom to the top along the tube. This crossflow configuration is advantageous in maintaining a constant temperature difference in heat transfer between the two fluids and maximizing the amount of heat transfer.

The molten salt on the tube side of the heat exchanger adopted the NaBF<sub>4</sub>-NaF system adopted by MSBR [6]. The thermal salt has excellent thermal properties and low cost.

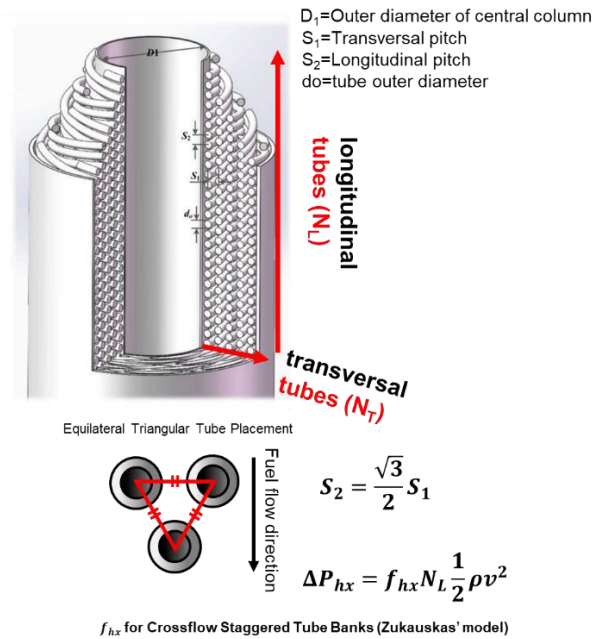


Figure 2 Helical coil heat exchanger model [10]

For this preliminary analysis, the adopted system parameters are summarized and listed in Table 1. At this time, the length of the heat exchanger area was determined according to the number of longitudinal tubes, and the diameter of the heat exchanger shell was determined through the number of transversal tubes.

**Table 1.** Design parameters of the PMFR system.

Parameters	Values
<b>Reactor</b>	
Helium injection rate	1 kg/sec
Core diameters	2 m
Core length	2 m
Riser diameters	1 m
Riser length	13 m
Core inlet-outlet temp.	600°C–750°C
<b>Fuel salt properties</b>	
UCl <sub>3</sub> –UCl <sub>4</sub> –KCl	
Salt composition	36.03%-9.1%-54.9% (mol)
Heat capacity	98.90 J/mol·K
UCl <sub>3</sub> [2]	129.7 J/mol·K
UCl <sub>4</sub>	Assumed (129.7 J/mol·K)
KCl [3]	73.6 J/mol·K
Viscosity [4]	3.5 cP – 2.0 cP
Density [4]	3142.5 kg/m <sup>3</sup> – 3003.3 kg/m <sup>3</sup>
Thermal conductivity	Assumed (0.5 W/mK)
<b>Heat exchangers</b>	
Helical coil	
Tubes outer diameter	25 mm
Tubes inner diameter	23 mm
Transversal P/D	2.0
Longitudinal P/D	$\sqrt{3}$
Numbers of modules	6 ea
Central column outer diameter	1 m
Transversal tube-rows	3 – 5
Longitudinal tube-rows	50 – 290
Tube conductivity	45 W/mK
<b>Thermal salt properties [6]</b>	
NaBF <sub>4</sub> -NaF	
Salt composition	92 % - 8 %
Heat capacity	1750 J/kgK
Viscosity	0.09 cP
Density	1507 kg/m <sup>3</sup>
Thermal conductivity	0.4 W/mK
Melting point	385 °C

The heat exchanger model was based on the imperial correlations using the research results of Zukauskas [7] for the shell side and Schmidt [8] for the tube side. The mass flow rate of the thermal salt on the secondary side was calculated based on the mass flow rate of the primary fuel salt, which is set to have the same heat capacity as the primary PMFR side. The iterative calculations were used to determine the secondary heat exchanger inlet temperature of thermal salt, which was adjusted to achieve the desired primary heat exchanger outlet temperature of 600°C.

#### 2.4 SCO<sub>2</sub> recompression cycle models

**Figure 3** depicts the arrangement of the recompression cycle. Our research team previously conducted a study on the SCO<sub>2</sub> recompression cycle analysis model and reported on its validation results [9]. The SCO<sub>2</sub> recompression cycle is an improvement over the simple recuperated SCO<sub>2</sub> cycle, as it utilizes an additional compression process. In a simple recuperated cycle, the SCO<sub>2</sub> that passes through the turbine is cooled through a recuperator and a pre-cooler before being compressed again. However, a pinch-point problem arises due to the variation in specific heat based on the pressure of SCO<sub>2</sub> in the recuperator. The recompression cycle resolves this specific heat mismatch by splitting the SCO<sub>2</sub> mass flow rate. It compresses a portion of the less cooled SCO<sub>2</sub>, thereby reducing the mass flow rate of the colder part with a relatively high specific heat value.

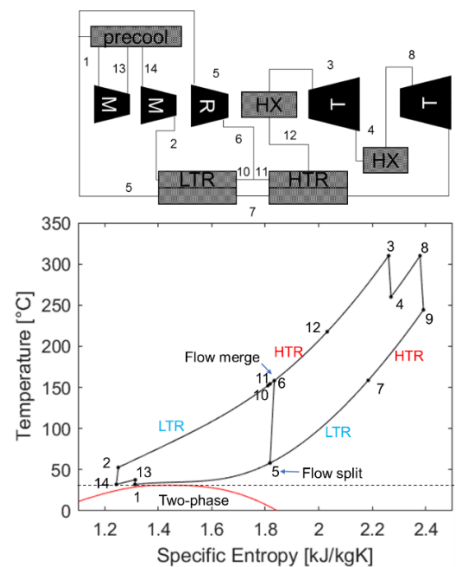


**Figure 3** SCO<sub>2</sub> recompression cycle with intercooling and reheating [9]

Based on the temperature range of the secondary system thermal salt obtained from the PMFR loop and heat exchanger model, the input values of the SCO<sub>2</sub> cycle analysis code, including the turbine inlet temperature and SCO<sub>2</sub> flow rate, were determined. The turbine inlet temperature was set to 10°C lower than the maximum temperature of the secondary system. The SCO<sub>2</sub> flow rate was calculated based on the amount of heat transferred from the intermediate heat exchanger. The mass split ratio and pressure ratio of the turbomachinery were optimized considering the maximum pressure and temperature. The cycle efficiency was calculated using the optimized mass split ratio and pressure ratio, and the electrical output was obtained by multiplying the PMFR fission heat and the efficiency.

**Table 2.** Parameters of the  $\text{SCO}_2$  recompression cycle.

Parameters	Values
Isentropic efficiency of compressors	0.85
Isentropic efficiency of turbine	0.92
Minimum pitch point temperature differences of the heat exchangers	10 °C
Compressor inlet temperature	32 °C
Turbine inlet pressure	25 MPa

### 3. Results & Discussion

**Figure 4** illustrates the heat transfer area per heat exchanger module, which varies based on the number of heat exchanger tubes. The diameter of the heat exchanger shell ranged from 1.3 m to 1.5 m depending on the number of transversal tubes, while the length of the heat exchanger varied from 2.2 m to 12.6 m depending on the number of longitudinal tubes.

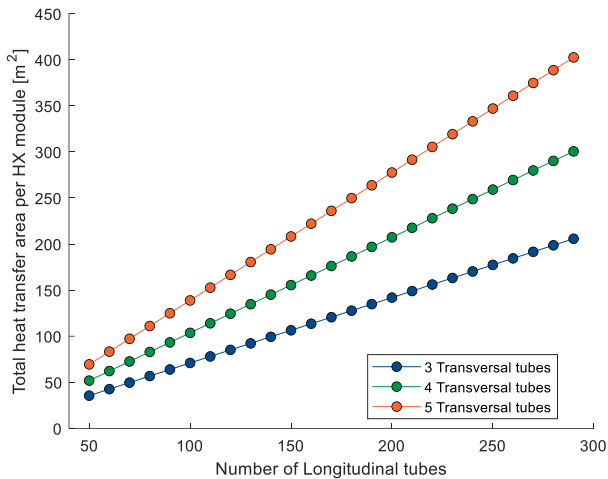


**Figure 4** Total heat transfer area of the heat exchanger module

The inlet and outlet temperatures of the tube-side thermal salt in each test matrix, calculated through the heat exchanger model, are illustrated in **Figure 5**. As the number of transversal tubes and longitudinal tubes of the heat exchanger increases, both exhibit an upward trend, which can be attributed to the increase in heat exchange area. However, as the number of longitudinal tubes rises, this upward trend gradually diminishes.

The thermodynamic efficiency of the  $\text{SCO}_2$  cycle, calculated with the temperature conditions of the thermal salt as input values, is presented in **Figure 6**. The trend of thermodynamic efficiency corresponds with the temperature change shown in **Figure 5**. Efficiency exceeds 50% in cases where the number of longitudinal tubes is 200 or more.

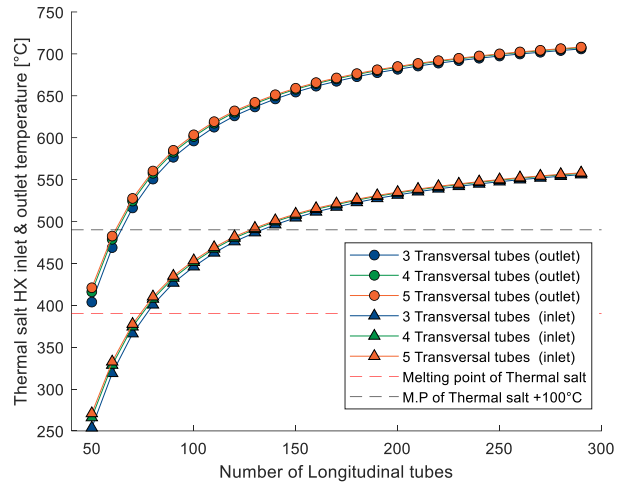


**Figure 5** Inlet and outlet temperature of the thermal salt

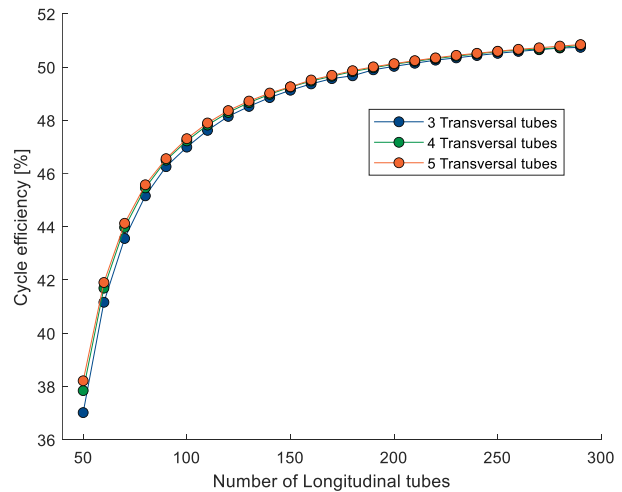


**Figure 6** Thermodynamic efficiency of the  $\text{SCO}_2$  cycle

**Figure 7** depicts the calculated PMFR fission heat and electric power. The results indicate that in all cases where the number of longitudinal tubes exceeds 70, reducing the natural circulation flow due to pressure loss in the PMFR loop has a greater impact than increasing the thermodynamic efficiency with the increase in longitudinal tubes. Additionally, the number of transversal tubes has a more significant impact on improving PMFR fission heat and electric power than longitudinal tubes. This is because the increase in the number of transversal tubes expands the effective area of the shell-side passage in the heat exchanger, reducing overall pressure loss and increasing the PMFR natural circulation flow rate.

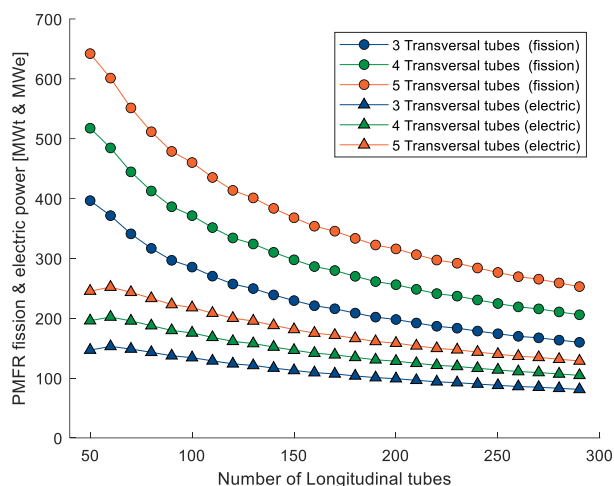


Figure 7 PMFR fission power and electric power

#### 4. Conclusion

In this study, the sensitivity analysis of the number of longitudinal and transversal tube arrangements of the helical coil heat exchanger was conducted. The PMFR natural circulation model was coupled with the  $\text{SCO}_2$  cycle model, and PMFR fission power and electric power were evaluated for the test matrix. When synthesizing the analysis results, it was confirmed that the number of transversal tubes contributed more to enhancing PMFR fission and electric power than the number of longitudinal tubes. In addition, it is noteworthy that the 200 longitudinal tubes and 5 transversal tubes cases calculated thermodynamic efficiency of 50% or more at an output of 300 MWt as a suitable power capacity. The results of this study can contribute to improving the feasibility of the conceptual design of PMFR, especially in terms of evaluating PMFR fission power and electric power.

#### Acknowledgments

This research was supported by the National Research Foundation of Korea (NRF) and funded by the ministry of Science, ICT, and Future Planning, Republic of Korea (grant numbers NRF-2021M2D2A2076382) and (No. NRF-2022M2D2A1A02061334).

#### REFERENCES

- [1] J. Lim, D. Shin, T. Kim, J. H. Park, J. Lee, Y. S. Cho, Y. Kim, S. Kim, S. J. Kim, Preliminary Analysis of the Effect of the Gas Injection on Natural Circulation for Molten Salt Reactor Type Small Modular Reactor System Operated without a Pump, Transactions of the Korean Nuclear Society Virtual Autumn Meeting October 21-22 (2021)
- [2] J. Fuger, V. B. Parker, W. N. Hubbard, F. L. Oetting, The chemical thermodynamics of actinide elements and compounds: Pt 8. The actinide halides, International Atomic Energy Agency, Vienna, (1983)

- [3] M.W. Chase, Jr., NIST-JANAF Thermochemical Tables, Fourth Edition, J.Phys. Chem. Ref. Data, Monograph 9, (1998).

- [4] S. Katyshev, Yu Chervinskii, V. Desyatnik. Density and viscosity of fused mixtures of uranium chlorides and potassium chloride. Atomic Energy, (1982).

- [5] R.W. Lockhart, R.W. Martinelli, Proposed correlation of data for isothermal twophase, two-component flow in pipes. Chem. Eng. Process. 45, 39–48, (1949).

- [6] Sabharwall, Piyush, et al. Process heat exchanger options for fluoride salt high temperature reactor. No. INL/EXT-11-21584. Idaho National Lab.(INL), Idaho Falls, ID (United States), (2011).

- [7] Zukauskas, A., and Romanas Ulinskas. "Heat transfer in tube banks in crossflow." (1988).

- [8] Schmidt, Eckehard F. "Wärmeübergang und druckverlust in rohrschlangen." Chemie Ingenieur Technik 39.13 (1967).

- [9] J.H. Lim, J.G Jeon, J.H Park, D.Y. Shin S.J. Kim, Thermodynamic study of  $\text{SCO}_2$  Recompression Brayton Cycle with Intercooling and Reheating for Light Water Reactor, Transactions of the Korean Nuclear Society Autumn Meeting, 2020

- [10] Sun, J., Zhang, R., Wang, M., Zhang, J., Qiu, S., Tian, W., & Su, G. (2022). Multi-objective optimization of helical coil steam generator in high temperature gas reactors with genetic algorithm and response surface method. Energy, 259.